*International Journal of Thermophysics, Vol. 25, No. 6, November 2004 (© 2004)*

# Experimental Determination of Isobaric Heat Capacities of R227 ($CF_3CHFCF_3$) from 223 to 283 K at Pressures up to 20 MPa.

**R. Hykrda,[1] J. Y. Coxam,[1,2] and V. Majer[1]**

*Received October 16, 2003*

A new experimental method for measuring isobaric heat capacity $c_p$ down to 223 K at pressures up to 30 MPa was developed with the aim to study alternative refrigerants at sub-ambient temperatures and elevated pressures. The experiments are carried out in a batch mode, using a differential fluxmetric calorimeter Setaram BT-215, equipped with a customized high-pressure unit. The measurements are performed at constant pressure with a continuous scan of temperature. First, the method was tested at atmospheric pressure with methanol in the temperature range 223–283 K. The relative deviation from recommended isobaric heat capacity data in the literature is about 0.5%. Second, the measurements were performed at pressure up to 18.2 MPa with an alternative refrigerant R134a (1,1,1,2-tetrafluoroethane) of well-known heat capacity. Our results agree with representative literature values within 0.4%. New original results were obtained for refrigerant R227 (1,1,1,2,3,3,3-heptafluoropropane) in the temperature range from 223 to 283 K and at pressures of 1.1, 5, 10, 15, and 20 MPa. The consistency of our isobaric heat capacities with calorimetric values above 273 K and with $pVT$ data reported in the literature is discussed.

**KEY WORDS:** alternative refrigerant; calorimetry; high pressure; isobaric heat capacity; low temperature; R134a; R227.

## 1. INTRODUCTION

Due to environmental regulations, the fully halogenated chlorofluorocarbon (CFC) refrigerants are being abandoned and replaced by hydrofluorocarbons (HFCs). For their applications in air-conditioning, refrigerating or

[1]Laboratoire de Thermodynamique des Solutions et des Polymères, UMR 6003 Université Blaise Pascal/CNRS, 24, Avenue des Landais, F-63177 Aubière, France.
[2]To whom correspondence should be addressed. E-mail: j-yves.coxam@univ-bpclermont.fr



0195-928X/04/1100-1677/0 

heat-pumping equipment, the behavior of these new refrigerants needs to be characterized over a wide range of temperatures and pressures. For this purpose, volumetric data and isobaric heat capacities are among the key thermophysical properties important for engineering calculations and for development of thermodynamic models. The latter data can be, in principle, calculated from spectroscopic ideal-gas heat capacities and a volumetric equation of state provided accurate $pVT$ data are available. This is, however, rarely the case, and new experimental data on thermal properties for alternative refrigerants are needed over an extended range of temperatures and pressures. This work presents a new calorimetric method for the determination of isobaric heat capacities at subambient temperatures and elevated pressures, data that are of practical interest particularly for heat transfer and energy efficiency calculations. Only very few direct heat capacity measurements at subambient temperatures have been performed for alternative refrigerants by now. We consider it useful to review the main data sources of heat capacities of refrigerants in the liquid state published in the literature over recent years.

The most extensive work in this field was performed in the Department of Mechanical Engineering at Keio University, Yokohama, Japan. A flow calorimeter [1–3] for measurements on freons at temperatures between 273 and 423 K and at pressures up to 3 MPa had a claimed uncertainty of 0.4%. This instrument was used for a considerable amount of data for several refrigerants: R114 (mixture of two isomers of dichlorotetrafluoroethane) [2,3], R134a (1,2,2,2-tetraflouroethane) [4,5], R123 (1,1-dichloro-2,2,2-trifluororoethane) [5], R142b (1-chloro-1,1-difluoroethane) [6], R152a (1,1-difluoroethane) [6], and R32 (difluoromethane) [7].

Two $C_p$ flow calorimeters for measurements on liquids, the first for pressures close to atmospheric ($p < 1$ MPa) [8] and the second for a wide pressure range up to 30 MPa [9], were developed by Ernst and collaborators in the Institute for Technical Thermodynamics at the University of Karlsruhe, Germany. Data with a claimed uncertainty of 0.1–0.2% were published for temperatures between 253 and 423 K for R227 (1,1,1,2,3,3,3-heptafluoropropane) [10] and between 253 and 523 K for R134a [11]. Low pressure measurements only ($p < 0.8$ MPa) were reported for R13 (trifluorochloromethane) and R23 (trifluoromethane) [12] in a limited temperature range from 273 to 373 K.

A different experimental approach was adopted by Magee at the National Institute of Standards and Technology, Boulder, Colorado, U.S.A. who constructed a batch calorimeter [13] for measurements of the isochoric heat capacity of a two-phase system where the liquid phase prevails. By conducting experiments under specified conditions, it is possible to obtain a number of thermodynamic quantities characterizing the studied system

and to derive the heat capacity of liquids along the saturation line with a claimed uncertainty to 0.7%. The data were published by Magee [14] for R134a at temperatures from 172 to 343 K and at pressures up to 35 MPa, and by Lüddecke and Magee [15] for R32 and R125 (pentafluoroethane) from subambient temperatures to 345 K and at pressures up to 35 MPa.

A new method for measuring the isobaric heat capacity $c_p$ of liquids at elevated temperatures and pressures was developed in our laboratory [16]. The experimental procedure uses a differential heat-flow calorimeter, C-80 model from Setaram (Lyon, France), equipped with a customized unit allowing measurements of heat capacity of a sample in a constant volume cell at isobaric conditions. This is possible due to communication of the cell with a large space outside the calorimeter filled with a gas at a selected pressure. In this way isobaric conditions are maintained throughout the experiment by expansion of the fluid from the calorimetric cell when the temperature is increased.

In this work, the procedure was adapted to measurements at subambient conditions using a low temperature Setaram BT-215 model. Instead of using the usual way of cooling the calorimeter by vaporization of nitrogen, a refrigerant liquid was supplied from a cryostat operating in a circuit with the calorimeter. This modification proposed by Polednicek and collaborators [17] made it easier to control the temperature of the calorimeter block (at a much lower cost). A new customized unit was designed for measuring the heat capacity at pressures up to 30 MPa. Due to significant thermal inertia observed for the BT-215 model, the previous operating mode in temperature steps [16] was replaced by a continuous scan of the temperature. The experimental method was tested at atmospheric pressure with methanol and at high pressures with the refrigerant R134a, comparing with representative recommended data from the literature [18, 19].

We have focused here on the alternative refrigerant R227 (1,1,1,2,3,3,3-heptafluoropropane), useful for substituting for R12 and R114 due to its similar normal boiling temperature ($T_{nbt} \approx 256$ K). This new refrigerant is convenient for use in units with high condensing temperatures like high-temperature heat pumps. Besides refrigeration applications, it is also useful in fire suppression and propellant applications. New experimental data on heat capacities are reported here at temperatures between 223 and 283 K and at pressures from 1 to 20 MPa. The consistency of our experimental isobaric heat capacities for R227 with the volumetric data of Klomfar et al. [20] was examined as well as comparisons with the $c_p$ data of Wirbser et al. [10] in the narrow range of conditions where these data overlap.

## 2. EXPERIMENTAL

The method involves extension towards lower temperatures and modification of a previously published technique [16] for measuring isobaric heat capacities of liquids at elevated pressures using Calvet type calorimeters. In order to carry out investigations at subambient temperatures, we used the BT-215 Setaram model, designed to work from 77 to 473 K. Both models, C-80 and BT-215, are differential fluxmetric calorimeters with a thermopile sensitivity of about $40\,\mu V \cdot mW^{-1}$. A Setaram G11 unit (Fig. 1) is used for controlling the temperature scan information, thermoregulation of the lid, and for retrieving and processing the calorimetric signal. The experiments are monitored by a microcomputer connected to the electronics of the G11 unit through an RS232 interface, which collects simultaneously the crucial experimental data: time, block temperature, and calorimetric signal.

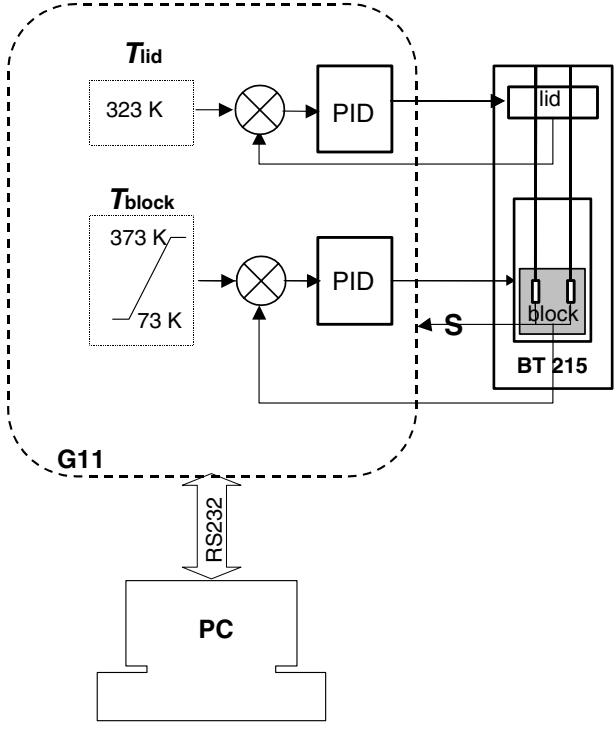


**Fig. 1.** Temperature control and data acquisition of the Setaram BT-215 calorimeter with the G11 unit. ($T_{lid}$) lid temperature, ($T_{block}$) calorimetric block temperature, ($S$) thermopile signal.

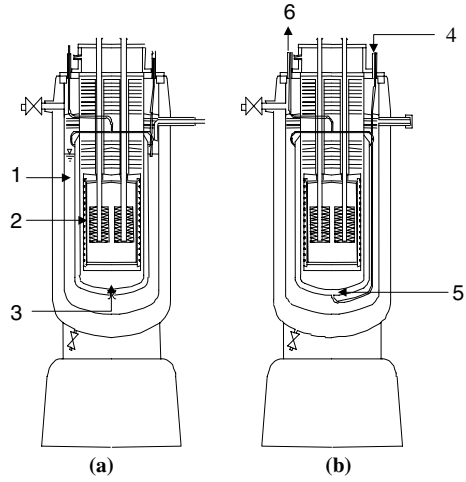


**Fig. 2.** Setaram BT-215 cooling systems using (a) vaporization of liquid nitrogen or (b) refrigerating liquid circulation. (1) liquid nitrogen reservoir, (2) calorimetric block, (3) liquid nitrogen inlet for vaporization, (4) refrigerating liquid input, (5) cooling jacket, (6) cooling jacket output.

In order to reach the lowest operating temperature (77 K), the BT-215 calorimeter was designed to be cooled by vaporization of liquid nitrogen placed in a jacket surrounding the calorimetric block (Fig. 2(a)). In this work, the experimental domain was, however, restricted to temperatures above 200 K since the data at lower temperatures are of little interest in the context of this investigation. It is therefore not necessary to use liquid nitrogen. The BT-215 cooling system was modified (Fig. 2(b)) to allow the circulation of an higher temperature cooling liquid (ethanol) around the block. The ethanol is supplied at a temperature of 210 K from the Lauda 200 cryostat. The refrigerant enters the calorimeter through a 6.35 mm o.d. tubing, soldered to the vaporization jacket inlet, flows around the calorimetric block, and exits the calorimeter at the top of the jacket, to be directed back to the cryostat. The calorimeter lid is controlled at 323 K to avoid any ice formation.

The calorimeter is equipped with a customized unit for measuring isobaric heat capacities of fluids (Fig. 3). Its main part consists of two cells, measuring and reference, made of Hastelloy cylinders (each with dimension of 18.6 mm o.d., 80 mm height, and 1 mm wall thickness) designed to sustain pressures up to 30 MPa. The measuring cell is filled and pressurized using two concentric tubes. The sample fluid enters the

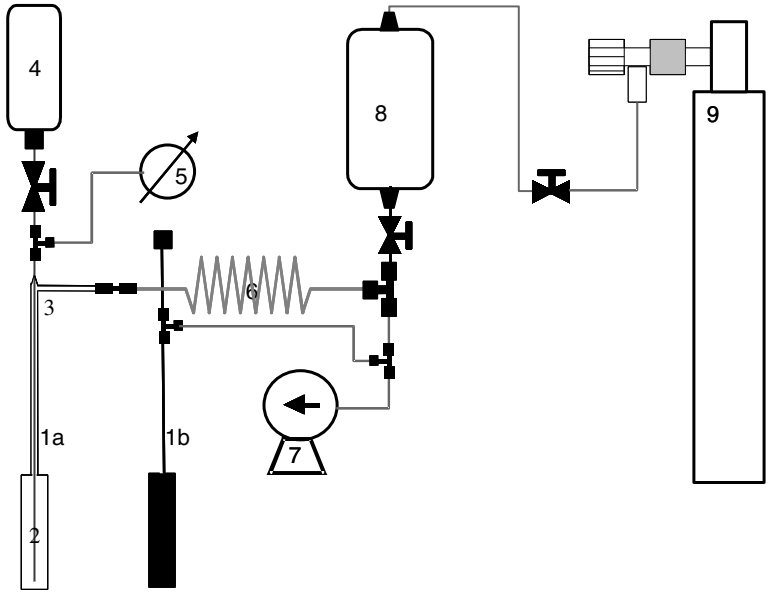


**Fig. 3.** High pressure unit with the filling and pressurizing system: (1a) measuring and (1b) reference cells, (2) inner filling tube, (3) lateral outlet, (4) sample storage tank, (5) pressure gauge, (6) gas-sample separation loop, (7) vacuum pump, (8) high-pressure buffer cylinder of 1 $dm^3$, (9) inert-gas high-pressure tank.

cell at the bottom level through an 1.58 mm o.d. inner tube and fills it entirely including the outer tube up to the output lateral connection. The filling is carried out with the help of a syringe when working with non-volatile liquids. More often, the fluid expands from a storage cylinder in the inner space of the unit previously evacuated. The working pressure is then adjusted with the help of a compressed inert gas (nitrogen or helium) which is contained in a temperature controlled high-pressure cylinder serving as a buffer volume compensating for the thermal expansion of the fluid. The pressure variation observed during the full temperature scan is less than 0.01 MPa. To prevent any contamination of the fluid by the inert gas dissolution, the gas–liquid interface has to be at a sufficient distance from the cell and the contact surface has to be minimized. The contact occurs in a gas-sample separation loop of 1.58 mm o.d., and 3 m length, connected to the cell via the lateral outlet. The pressure is measured with a Druck (DPI 260) pressure gauge (0.1–40 MPa) with an uncertainty of 0.15% of the full pressure range, and with a resolution of 0.01 MPa. The pressure gauge has been calibrated, and the precision is 0.02%. During a temperature scan, a small pressure variation of about

0.01 MPa is observed; this pressure change occurred over a 24 h run, so no significant perturbation of the calorimetric signal was detected.

The isobaric heat capacities are derived from measurements of the heat power $\dot{q}$ (in mW) exchanged between the system and the calorimetric block when heating or cooling. The heat power is detected by a thermopile surrounding the cell, consisting of a large number of thermocouples connected in series. The temperature difference between the block and the cell induces an electric potential $E$ (in $\mu$V); the sensitivity ratio $E/\dot{q}$ is determined by a Joule effect calibration. The heat power $\dot{q}$ for one cell can be considered as the sum of two terms: one related to the specific heat of the sample fluid $c_{p,f}$ and the second to the specific heat of the cell itself $c_c$ The overall heat exchanged is obtained by integration in time $\tau$ over successive temperature increments ($\Delta T$)

$$Q = \int_{\tau_T}^{\tau_{T+\Delta T}} \dot{q}\, d\tau = \int_{\tau_T}^{\tau_{T+\Delta T}} (\dot{q}_{\text{fluid}} + \dot{q}_{\text{cell}})\, d\tau = \int_{T}^{T+\Delta T} (m_f c_f + m_c c_c)\, dT, \qquad (1)$$

where $m_f$ and $m_c$ represent the masses of the fluid and the cell, respectively. Our method takes into account the thermal expansion of the fluid when heating the cell at a constant pressure. The mass of the fluid $m_f$ is then expressed as the product of the constant inner cell volume $V_c$ and the temperature-dependent density $\rho_f$. In the step method, reported earlier [16], the signal is integrated between baseline signals determined from equilibrium states at an initial ($T$) and a final ($T + \Delta T$) temperature. The thermal inertia observed with the BT-215 calorimeter induces important delays in reaching temperature equilibria which results in an important increase of the experiment time. For that reason it was necessary to change the experimental mode to a continuous scan in temperature. Then the full temperature range is scanned at a constant rate $\delta T/\delta\tau$, and the isobaric heat capacity is derived directly from the heat power $\dot{q}$.

For differential detection, the signal is related to the heat power difference between the measuring cell $\dot{q}_m$ filled with the investigated fluid and an empty reference cell $\dot{q}_r$:

$$\dot{q}_{\text{diff}}(\text{fluid}) = \dot{q}_m - \dot{q}_r = [V_{c,m}\rho_f c_{p,f} + (V_c\rho_c c_c)_m - (V_c\rho_c c_c)_r]\delta T/\delta\tau. \qquad (2)$$

For obtaining the isobaric heat capacity of the investigated fluid $c_{p,f}$, it is necessary to perform two additional experiments at the same scanning rates. First, a blank experiment is performed with both the measuring and reference cells empty which reflects the difference in the thermal response of the cells.

$$\dot{q}_{\text{diff}}(\text{blank}) = [(V_c\rho_c c_c)_m - (V_c\rho_c c_c)_r]\delta T/\delta\tau. \qquad (3)$$

Second, a calibration experiment is carried out with a fluid of well known heat capacity $c_{p,cal}$ and density $\rho_{cal}$ over the complete temperature range of measurements

$$\dot{q}_{diff}(cal) = [V_{c,m}\rho_{cal}c_{p,cal} + (V_c\rho_c c_c)_m - (V_c\rho_c c_c)_r]\delta T/\delta\tau. \quad (4)$$

Then the volume $V_c$ can be obtained from the combination of Eqs. (3) and (4) as follows

$$V_{c,m} = \frac{\dot{q}_{diff}(cal) - \dot{q}_{diff}(blank)}{\rho_{cal}c_{p,cal}\delta T/\delta\tau}. \quad (5)$$

It should be stressed that $V_{c,m}$ should not be regarded as the physical volume of the measuring cell, which is difficult to define exactly due to the communication with the outside space. It is rather a general calibration constant of the experiment which changes slightly with temperature and is generally independent of pressure. Once the $V_{c,m}$ constant is determined, it is possible to calculate the specific isobaric heat capacity as

$$c_{p,f} = \frac{\dot{q}_{diff}(fluid) - \dot{q}_{diff}(blank)}{V_{c,m}\rho_f\delta T/\delta\tau}. \quad (6)$$

It is apparent from this equation that the investigated fluid density must be accurately known over the temperature and pressure range of the calorimetric experiments. No data are necessary regarding the reference cell.

The scanning rate is set to $0.05\,K\cdot min^{-1}$. A platinum resistance thermometer located in the calorimeter between the two cells measures the temperature $T$. The choice of the scanning rate value was affected by the necessity to minimize the length of the initial phase of the experiment, when the temperature increase is not regular (see Fig. 4). This transition range is usually 10 K before the regular temperature change is attained. The exact scanning rate value $\delta T/\delta\tau$ is determined as a function of temperature from the registered temperature and time signals. It is generally constant within 0.05% during the whole experiment with the exception of the initial phase. The uncertainty in the scanning rate (see Eqs. (5) and (6)) can be neglected in comparison with other error sources.

The calibration experiments to determine the cell volume $V_{c,m}$ were carried out with ethanol, in the temperature range from 220 to 290 K and at atmospheric pressure. Isobaric heat capacities from the critical compilation by Zábranský et al. [18] and densities recommended by Cibulka [21] were used. The calibration experiments were periodically repeated, and $V_{c,m}$ was calculated as a function of temperature with a step of 5 K; the values plotted in Fig. 5 correspond to the average of several measurements. The values of $V_{c,m}$ determined by calorimetric measurements take also into

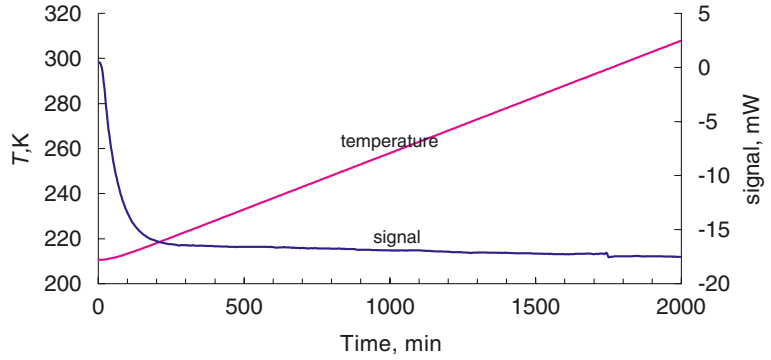


**Fig. 4.** Differential calorimetric signal and block temperature versus time when heating at a constant scanning rate of 0.05 K·min$^{-1}$, from 210 to 303 K, with the measuring cell filled with a liquid sample.

account the external perturbations that are not compensated by the differential arrangement. The moderate fluctuations around average values are mainly due to heat leaks caused by the temperature gradient along the filling tubes and depend also on the room temperature. Other perturbations can be caused by small changes in the thermal contact of the measuring and reference cells inside the thermopile well of the calorimeter. The average value

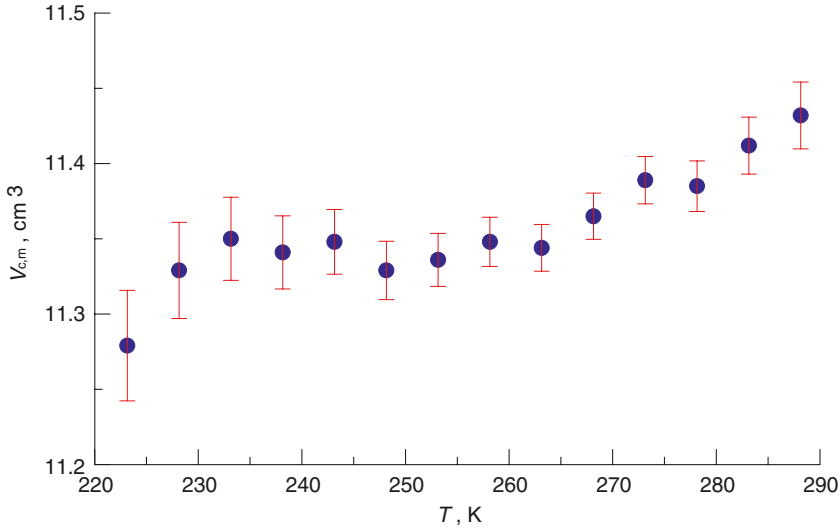


**Fig. 5.** Average $V_{c,m}$ constant for the measuring cell between 220 and 290 K, obtained by calibration experiment.

is relatively constant for temperatures between 223 and 273 K, as shown in Fig. 5. Below 223 K, the higher scatter of values is due to the transition phase. Above 273 K the measurements are perturbed by the temperature regulation instability observed when the temperature difference between the block and the refrigerant fluid is significant. The relative error of $V_{c,m}$ due to these perturbations is estimated to be 0.2% between 223 and 273 K. The total uncertainty of 0.4% estimated for $V_{c,m}$ includes the ethanol density and heat capacity errors estimated to be 0.1 and 0.2%, respectively. In Eq. (6), the signal difference ($\dot{q}_{diff}$(fluid) $-$ $\dot{q}_{diff}$(blank)) and the density of a fluid (methanol or refrigerant) are known with relative errors of 0.3 and 0.1%, respectively. Thus, the total probable uncertainty of the measured isobaric heat capacities of studied compounds is estimated to be 0.5%.

The fluids used in the test experiments and for calibration were from Acrōs organics with a purity of 99.8% for methanol and from Prolabo with a purity of 99.85% for ethanol. The refrigerants R134a and R227 with a purity of 99.9%, used in this work, were provided by Solvay.

## 3. RESULTS

The experimental procedure was tested first at atmospheric pressure with methanol in the temperature range 223–283 K. The recommended values of isobaric heat capacities and densities of methanol are available from Zábranský et al. [18] and Cibulka [21], respectively. The heat capacity results are presented in Table I with the percentage deviations of our experimental values from the literature; the average deviation is 0.38%.

In the next step, the test of the experimental procedure was performed at high pressure with refrigerant R134a ($T_c = 374$ K, $p_c = 4.06$ MPa) for which the isobaric heat capacity and density values were generated from the fundamental equation of state by Tillner-Roth and Baehr [19]. Our measurements were carried out in the liquid phase at temperatures between 223 and 278 K and at constant pressures of 0.75, 5, 10, and 18.2 MPa. The lowest pressure corresponds to that in the storage cylinder from which R134a is supplied under its vapor pressure. To insure a constant pressure, the storage cylinder ($V = 500$ cm$^3$) was thermo-regulated at a constant temperature slightly above that of the laboratory. At higher pressures, the liquid was pressurized by use of nitrogen. Our isobaric heat capacity data have been compared, in the temperature range from 220 to 270 K at pressure of 10 MPa, with the isochoric heat capacity $C_v$ data of Magee [14]. At these temperatures and pressure, it is possible to convert simply the isochoric heat capacity to isobaric using the differences $C_p - C_V$ tabulated for R134a by Tillner-Roth and Baehr [19]. The average deviation between our experimental $c_p$ results and the values obtained from the

**Table I.** Experimental Isobaric Heat Capacities of Methanol at Atmospheric Pressure; New Experimental Values $c_{p\ exp}$ Compared with the Data $c_{p\ lit}$ Recommended by Zábranský et al. [18]

| T(K) | $c_{pexp}(J\cdot K^{-1}\cdot g^{-1})$ | $c_{plit}(J\cdot K^{-1}\cdot g^{-1})$ | $\delta_r c_p(\%)$ |
|---|---|---|---|
| 223.15 | 2.238 | 2.247 | −0.41 |
| 228.15 | 2.250 | 2.256 | −0.27 |
| 233.15 | 2.256 | 2.266 | −0.44 |
| 238.15 | 2.268 | 2.277 | −0.37 |
| 243.15 | 2.287 | 2.289 | −0.11 |
| 248.15 | 2.304 | 2.303 | 0.02 |
| 253.15 | 2.326 | 2.319 | 0.30 |
| 258.15 | 2.344 | 2.336 | 0.36 |
| 263.15 | 2.363 | 2.354 | 0.35 |
| 268.15 | 2.378 | 2.375 | 0.14 |
| 273.15 | 2.389 | 2.396 | −0.33 |
| 278.15 | 2.402 | 2.420 | −0.73 |
| 283.15 | 2.437 | 2.445 | −0.32 |

isochoric heat capacities of Magee [14] is 0.3%. The average deviations between the data of Magee and the recommended values of Tillner-Roth and Baehr [19] are about 0.1%. Then we consider that the comparison of our isobaric heat capacities, with the recommended values of Tillner-Roth and Baehr [19] in Table II is sufficient, considering the experimental uncertainty of our data. The average deviation is comparable with that observed for methanol, 0.5% at a pressure of 0.75 MPa and decreasing to 0.3% at higher pressures, for temperatures up to 278 K. The maximum percentage deviations are observed at the extremes of the experimental temperature range where the results of measurements are affected by inadequacies in the temperature control; this is particularly true for temperatures above 278 K for which we have not taken into consideration when calculating the average deviations from the literature data. A stringent test is a comparison of the pressure effect on the isobaric heat capacity with the temperature effect on the volume according to the thermodynamic relationship

$$\left(\frac{\partial c_p}{\partial p}\right)_T = -T\left(\frac{\partial^2 v}{\partial T^2}\right)_p, \tag{7}$$

where $v$ is the specific volume. The first pressure derivative of $c_p$ was calculated from a second-order polynomial function $c_p = f(p)$ fitted to our experimental points, and the second temperature derivative of volume was obtained from the fundamental equation of Tillner-Roth and Baehr [19].

**Table II.** Experimental Isobaric Heat Capacities of R134a ($M_w = 102.03\,g{\cdot}mol^{-1}$) at High Pressures; New Experimental Values $c_{p\ exp}$ Compared with the Values $c_{p\ lit}$ Generated from Equation of Tillner-Roth and Baehr [19].

| T(K) | $c_{p\ exp}$ ($J{\cdot}K^{-1}g^{-1}$) | $c_{p\ lit}$ ($J{\cdot}K^{-1}{\cdot}g^{-1}$) | $\delta c_p$ ($J{\cdot}K^{-1}{\cdot}g^{-1}$) | $\delta_r c_p$ (%) | $c_{p\ exp}$ ($J{\cdot}K^{-1}{\cdot}g^{-1}$) | $c_{p\ lit}$ ($J{\cdot}k^{-1}{\cdot}g^{-1}$) | $\delta c_p$ ($J{\cdot}K^{-1}{\cdot}g^{-1}$) | $\delta_r c_p$ (%) |
|---|---|---|---|---|---|---|---|---|
| $p = 0.75$ MPa | | | | | $p = 5.0$ MPa | | | |
| 223.15 | 1.229 | 1.237 | −0.008 | −0.62 | 1.232 | 1.230 | 0.003 | 0.22 |
| 228.15 | 1.245 | 1.245 | 0.000 | 0.01 | 1.238 | 1.237 | 0.001 | 0.06 |
| 233.15 | 1.254 | 1.253 | 0.001 | 0.09 | 1.245 | 1.245 | 0.000 | 0.01 |
| 238.15 | 1.265 | 1.262 | 0.003 | 0.26 | 1.254 | 1.253 | 0.001 | 0.09 |
| 243.15 | 1.272 | 1.271 | 0.001 | 0.07 | 1.262 | 1.261 | 0.001 | 0.10 |
| 248.15 | 1.283 | 1.281 | 0.002 | 0.19 | 1.268 | 1.269 | −0.001 | −0.08 |
| 253.15 | 1.292 | 1.291 | 0.001 | 0.10 | 1.275 | 1.278 | −0.003 | −0.26 |
| 258.15 | 1.308 | 1.302 | 0.006 | 0.47 | 1.284 | 1.288 | −0.004 | −0.31 |
| 263.15 | 1.319 | 1.313 | 0.006 | 0.42 | 1.293 | 1.297 | −0.004 | −0.31 |
| 268.15 | 1.333 | 1.325 | 0.008 | 0.60 | 1.302 | 1.308 | −0.006 | −0.46 |
| 273.15 | 1.344 | 1.339 | 0.005 | 0.41 | 1.310 | 1.318 | −0.008 | −0.61 |
| 278.15 | 1.369 | 1.353 | 0.016 | 1.19 | 1.316 | 1.330 | −0.014 | −1.05 |
| 283.15 | 1.453 | 1.368 | 0.085 | 6.22 | 1.322 | 1.342 | −0.020 | −1.47 |
| $p = 10.0$ MPa | | | | | $p = 18.2$ MPa | | | |
| 223.15 | 1.229 | 1.223 | 0.006 | 0.50 | 1.203 | 1.213 | −0.010 | −0.83 |
| 228.15 | 1.232 | 1.229 | 0.003 | 0.24 | 1.218 | 1.219 | −0.001 | −0.10 |
| 233.15 | 1.239 | 1.236 | 0.003 | 0.22 | 1.226 | 1.225 | 0.001 | 0.07 |
| 238.15 | 1.244 | 1.243 | 0.000 | 0.03 | 1.233 | 1.231 | 0.002 | 0.16 |
| 243.15 | 1.251 | 1.251 | 0.001 | 0.06 | 1.238 | 1.238 | 0.000 | 0.03 |
| 248.15 | 1.260 | 1.258 | 0.001 | 0.10 | 1.245 | 1.244 | 0.001 | 0.08 |
| 253.15 | 1.267 | 1.266 | 0.001 | 0.10 | 1.254 | 1.251 | 0.003 | 0.24 |
| 258.15 | 1.276 | 1.274 | 0.002 | 0.17 | 1.258 | 1.258 | 0.001 | 0.05 |
| 263.15 | 1.285 | 1.283 | 0.002 | 0.16 | 1.265 | 1.265 | 0.001 | 0.06 |
| 268.15 | 1.295 | 1.291 | 0.004 | 0.28 | 1.273 | 1.272 | 0.001 | 0.06 |
| 273.15 | 1.306 | 1.300 | 0.005 | 0.40 | 1.278 | 1.279 | −0.001 | −0.07 |
| 278.15 | 1.309 | 1.310 | 0.000 | −0.04 | 1.279 | 1.287 | −0.008 | −0.61 |
| 283.15 | 1.302 | 1.320 | −0.017 | −1.31 | 1.261 | 1.294 | −0.034 | −2.61 |

Considering the small pressure effect observed on the isobaric heat capacities, the pressure derivatives calculated for several temperatures at 10 MPa (Fig. 6) show good consistency (differences less than 5%) with the temperature derivatives of the volumetric data.

The isobaric heat capacities of refrigerant R227 were measured from 223 to 283 K at pressures of 1.1, 5, 10, 15, and 20 MPa where the refrigerant is always liquid ($T_c = 375.1$ K, $p_c = 2.95$ MPa). The cell was pressurized by using nitrogen, except at a pressure of 1.1 MPa, where the refrigerant is under its saturation vapor pressure at the storage cylinder

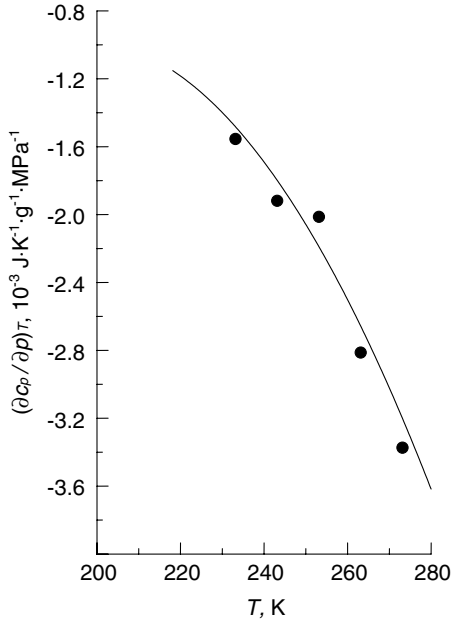


**Fig. 6.** Pressure derivatives $(\partial c_p/\partial p)_T$ of our $c_p$ values for R134 at 10 MPa (•) compared with the terms $-T(\partial^2 V/\partial T^2)_p$ calculated from the fundamental equation of state by Tillner-Roth and Baehr [19] (—).

temperature. The R227 densities were obtained from the $pVT$ equations of Klomfar et al. [20]. Our experimental isobaric heat capacities were fitted to a second-order polynomial function over the full temperature range; the adjustable parameters are listed in Table III. The experimental and fitted isobaric heat capacities are listed in Table IV and plotted versus temperature in Fig. 7. The average deviation of the fit is between 0.5 and 0.3%. The experimental isobaric heat capacity isotherms are also plotted as a function of pressure in Fig. 8, together with the data of Wirbser

**Table III.** Coefficients of the Polynomial Function $c_p = a + b(T/100) + c(T/100)^2$ Fitting the New Data for R227

| $p$(MPa) | 1.1 | 5 | 10 | 15 | 20 |
|---|---|---|---|---|---|
| $a$(J·K$^{-1}$· g$^{-1}$) | 1.53233 | 1.44115 | 0.910227 | 0.948743 | 1.26213 |
| $b$(J·K$^{-2}$· g$^{-1}$) | −0.552059 | −0.47203 | −0.0404712 | −0.06771 | −0.314658 |
| $c$(J·K$^{-3}$· g$^{-1}$) | 0.145745 | 0.126856 | 0.0377639 | 0.0414919 | 0.0885116 |

**Table IV.** Experimental Isobaric Heat Capacities of R227 ($M_w = 170.03\,g{\cdot}mol^{-1}$) at High Pressures; New Experimental Values $c_{p\ exp}$ Compared with the Values $c_{p\ fit}$ Generated from the Fitting Equation (Table III).

| $T(K)$ | $c_{p\ exp}$ ($J{\cdot}K^{-1}{\cdot}g^{-1}$) | $c_{p\ fit}$ ($J{\cdot}K^{-1}{\cdot}g^{-1}$) | $\delta_r c_p$ (%) | $c_{p\ exp}$ ($J{\cdot}K^{-1}{\cdot}g^{-1}$) | $c_{p\ fit}$ ($J{\cdot}K^{-1}{\cdot}g^{-1}$) | $\delta_r c_p$ (%) |
|---|---|---|---|---|---|---|
| $p = 1.1$ MPa | | | | $p = 5$ MPa | | |
| 223.15 | 1.031 | 1.026 | 0.47 | 1.004 | 1.020 | −1.53 |
| 228.15 | 1.027 | 1.031 | −0.43 | 1.021 | 1.025 | −0.34 |
| 233.15 | 1.037 | 1.037 | −0.04 | 1.033 | 1.030 | 0.27 |
| 238.15 | 1.046 | 1.044 | 0.17 | 1.039 | 1.036 | 0.24 |
| 243.15 | 1.052 | 1.052 | 0.03 | 1.044 | 1.043 | 0.06 |
| 248.15 | 1.057 | 1.060 | −0.27 | 1.049 | 1.051 | −0.19 |
| 253.15 | 1.066 | 1.069 | −0.26 | 1.060 | 1.059 | 0.08 |
| 258.15 | 1.078 | 1.078 | −0.04 | 1.067 | 1.068 | −0.09 |
| 263.15 | 1.087 | 1.089 | −0.17 | 1.077 | 1.077 | −0.04 |
| 268.15 | 1.101 | 1.100 | 0.09 | 1.088 | 1.088 | 0.041 |
| 273.15 | 1.118 | 1.112 | 0.56 | 1.097 | 1.098 | −0.12 |
| 278.15 | | | | 1.110 | 1.110 | 0.03 |
| $p = 10$ MPa | | | | $p = 15$ MPa | | |
| 223.15 | 0.998 | 1.008 | −0.99 | 0.998 | 1.004 | −0.62 |
| 228.15 | 1.014 | 1.014 | −0.05 | 1.009 | 1.010 | −0.12 |
| 233.15 | 1.022 | 1.021 | 0.08 | 1.017 | 1.016 | 0.06 |
| 238.15 | 1.030 | 1.028 | 0.19 | 1.023 | 1.023 | 0.02 |
| 243.15 | 1.034 | 1.035 | −0.10 | 1.029 | 1.029 | −0.04 |
| 248.15 | 1.040 | 1.042 | −0.22 | 1.038 | 1.036 | 0.17 |
| 253.15 | 1.048 | 1.050 | −0.17 | 1.045 | 1.043 | 0.17 |
| 258.15 | 1.058 | 1.057 | 0.05 | 1.051 | 1.050 | 0.05 |
| 263.15 | 1.067 | 1.065 | 0.17 | 1.056 | 1.058 | −0.18 |
| 268.15 | 1.075 | 1.073 | 0.16 | 1.062 | 1.066 | −0.33 |
| 273.15 | 1.082 | 1.081 | 0.05 | 1.073 | 1.073 | −0.03 |
| 278.15 | 1.088 | 1.090 | −0.17 | 1.084 | 1.081 | 0.24 |
| 283.15 | 1.101 | 1.098 | 0.24 | 1.088 | 1.090 | −0.15 |
| $p = 20$ MPa | | | | | | |
| 223.15 | 0.991 | 1.001 | −0.98 | | | |
| 228.15 | 1.002 | 1.005 | −0.30 | | | |
| 233.15 | 1.011 | 1.010 | 0.13 | | | |
| 238.15 | 1.017 | 1.015 | 0.22 | | | |
| 243.15 | 1.021 | 1.020 | 0.06 | | | |
| 248.15 | 1.026 | 1.026 | −0.03 | | | |
| 253.15 | 1.035 | 1.033 | 0.21 | | | |
| 258.15 | 1.040 | 1.040 | 0.03 | | | |
| 263.15 | 1.045 | 1.047 | −0.19 | | | |
| 268.15 | 1.051 | 1.055 | −0.36 | | | |
| 273.15 | 1.062 | 1.063 | −0.10 | | | |
| 278.15 | 1.075 | 1.072 | 0.31 | | | |
| 283.15 | 1.081 | 1.081 | 0.02 | | | |

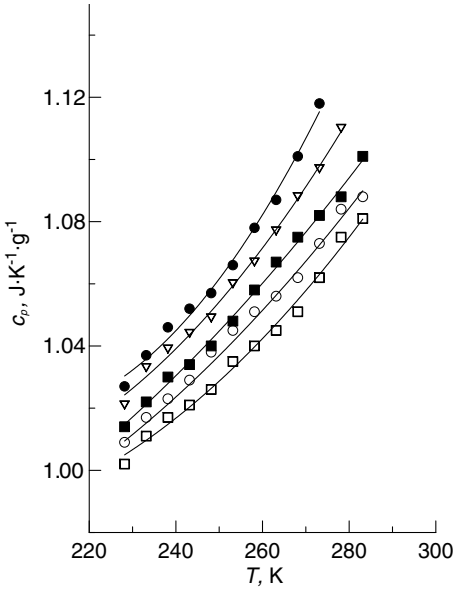


**Fig. 7.** Experimental isobaric heat capacities of R227 at 1.1 MPa (●), 5 MPa (▽), 10 MPa (■), 15 MPa (○), 20 MPa (□), and polynomial fits (—).

et al. [10] at 273, 288, and 303 K. The two data sets seem to be reasonably consistent in the region, where they overlap with the exception of values at 273.15 K where a significant difference is apparent between the data of this study and those of Wirbser et al. Both data sets follow the same trend when plotted as a function of temperature as shown in Fig. 9 for pressures of 10 and 15 MPa. The values of Wirbser et al. at 273 K are, however, at both pressures different from our polynomial fit, which otherwise represents satisfactorily our data and the data of Wirbser et al. at two higher temperatures. In order to test the consistency more extensively, as in the case of R134a, the pressure dependence of the isobaric heat capacities was compared with the temperature dependence of the specific volumes (see Eq. (7)) using the volumetric data of Klomfar et al. [20]. The derivatives reported at pressure of 10 MPa (Fig. 10) show good agreement between calorimetric and volumetric data with some differences at 273 K for the Wirbser et al. heat capacity and at 283 K for our experimental value. There comparisons suggest that the Wirbser et al. data at 273 K might seem to have higher uncertainty compared to measurements at higher temperatures.

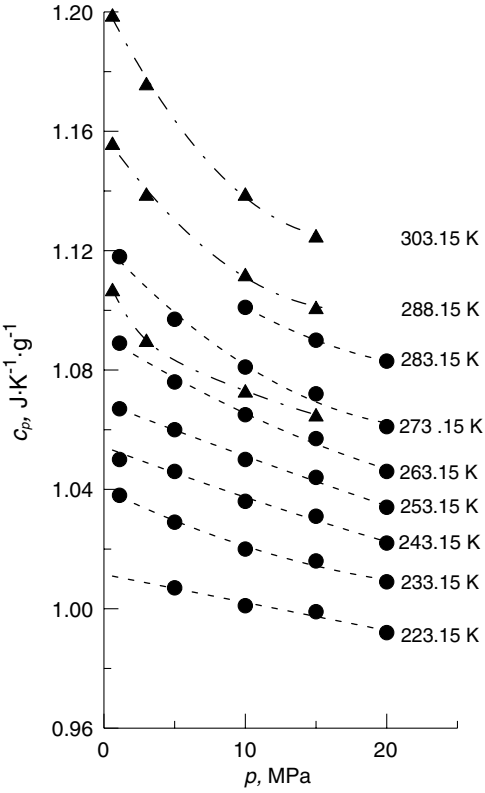


**Fig. 8.** Experimental isotherms of $c_p$ for R227 between 1 and 20 MPa, this work (●, ---) and Wirbser et al. [10] (▲, – — –).

This investigation has shown that it is possible to measure with the proposed method the isobaric heat capacities of refrigerants with an uncertainty around 0.5% in the temperature range between 220 and 280 K. The uncertainty is probably somewhat higher (1%) at the lowest temperature and when approaching room temperature due to difficulties to control the experiment in the initial phase and at ambient temperature conditions. The time to reach a constant scanning rate at the beginning of an experiment is related to the calorimetric block inertia; this time is minimized by selecting a small scanning rate. The advantage is the possibility to conduct the high pressure experiments with fluids in a fully automated mode using a commercially available calorimeter Setaram BT-215 equipped with a customized unit which is relatively easy to construct. Comparisons with the independent calorimetric results and good consistency with volumetric

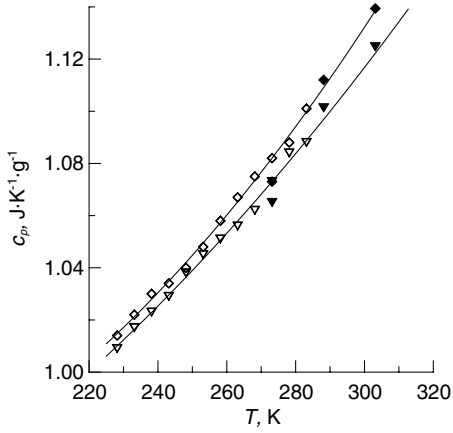


**Fig. 9.** Experimental isobaric heat capacities of R227 measured in this work at: 10 MPa (◇), 15 MPa (▽) and reported by Wirbser et al. [10] at: 10 MPa (♦),15 MPa (▼).

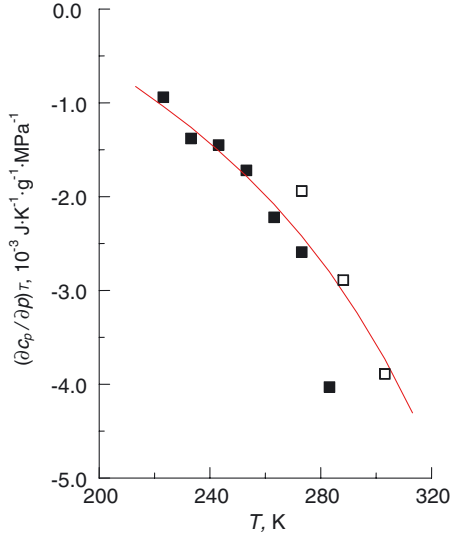


**Fig. 10.** Pressure derivatives $(\partial c_p/\partial P)_T$ of $c_p$ values from this work (□) and of Wirbser et al. [10] (■) for R227 at 10 MPa compared with the terms $-T(\partial^2 V/\partial T^2)_P$ calculated from the volumetric data by Klomfar et al. [20] (—).

measurements make us believe that our data are not subject to any significant systematic errors. Improvement of the operation at temperatures above 273 K is, however, desirable.

## REFERENCES


1. A. Saitoh, H. Sato, and K. Watanabe, *Int. J. Thermophys*. **10**:649 (1989).
2. M. Ashizawa, A. Saitoh, and A. Sato, in *Proc. 17th Int. Congress Refrig.,* Vol. B, Paris, Int. Inst. Refrig. (1987), p. 185.
3. H. Sato, N. Sakate, M. Ashizawa, M. Uematsu, and K. Watanabe, in *Proc. 2nd ASME-JSME Thermal Eng. Joint Conf.,* Vol. 4, P. J. Marto and I. Tanasawa, eds. (ASME, New York, 1987), p. 351.
4. A. Saitoh, S. Nakawaga, H. Sato, and K. Watanabe, *J. Chem. Eng. Data* **35**:107 (1990).
5. S. Nakagawa, H. Sato, and K. Watanabe, *High Temp. - High Press.* **23**:191 (1991).
6. S. Nakagawa, T. Hori, H. Sato, and K. Watanabe, *J. Chem. Eng. Data.* **38**:70 (1993).
7. M. Yomo, H. Sato, and K. Watanabe, *High Temp. - High Press.* **26**:267 (1994).
8. G. Ernst, G. Bräuning, and J.-F. Lai, *Can. J. Chem*. **66**:999 (1988).
9. G. Ernst, G. Maurer, and E.Wiederuh, *J. Chem. Thermodyn.* **21**:53 (1989).
10. H. Wirbser, G. Brauning, J. Gurtner, and G. Ernst, *J. Chem. Thermodyn*. **24**:761 (1992).
11. G. Ernst, J. Gürtner, and H. Wirbser, *J. Chem. Thermodyn*. **29**:1113 (1997).
12. G. Ernst, J. Gürtner, and H. Wirbser, *J. Chem. Thermodyn* **29**:1125 (1997).
13. J. W. Magee, *J. Res. Nat. Inst. Stand. Technol.* **96**:725 (1991).
14. J. W. Magee, *Int. J. Refrig.* **15**:372 (1992).
15. T. O. Lüddecke and J. W. Magee, *Int. J. Thermophys*. **17**:823 (1996).
16. J.-Y. Coxam, J. R. Quint, and J.-P. E. Grolier, *J. Chem. Thermodyn*. **23**:1075 (1991).
17. M. Polednicek, *Ph.D. Thesis* (Blaise Pascal University, Clermont-Ferrand and Prague Institute of Chemical Technology 2000).
18. M. Zábranský, V. Ružicka, V. Majer, and E. S. Domalski, *Heat Capacity of Liquids*, Vols. I and II, *J. Phys. Chem. Ref. Data*, Monograph No. 6, (Washington, D.C., 1996).
19. R. Tillner-Roth and H. D. Baehr, *J. Phys. Chem. Ref. Data* **23**:657 (1994).
20. J. Klomfar, J. Hrubý, and O. Šifner, *J. Chem. Thermodyn*. **26**:965 (1994).
21. I. Cibulka, *Fluid Phase Equilib.* **89**:1 (1992).